Effect of Non Newtonian Fluid on the Kerf Angle of a Dailatant Jet

Hassan Omrani[1,*], Hadi Jafari[2], Abozar Karimpour[1]

[1.] Department of Mechanical Engineering, Allame Amini High Educational, Institute of Bahnamir, Mazandaran, Iran
[2.] Department of Mechanical Engineering, Ayatollah Amoli Branch, Islamic Azad University, Amol, Iran

Abstract: The result of liquid properties after adding cornstarch additives on the stability of an abrasive dilatant jet (ADJ) is presented and discussed with a view to enhance the jet stability for ADJ machining. It is shown that jet disintegration is a result of the jet internal disturbances associated with the fluid properties and the external air friction acting upon the jet surface. A jet becomes more stable with the addition of cornstarch additives, which is found to be mainly attributed to the increase of fluid viscosity. By contrast, the surrounding air friction with the jet results in the jet to disintegrate, and this external effect increases with an increase in the jet velocity. The developed model is finally verified experimentally, which shows that the model predictions are in good agreement with the experimental data [1].

1. Introduction

The abrasive waterjet (AWJ) technology has received considerable attention from industry owing to its beneficial characteristics in the machining of various materials, particularly difficult-to-machine and thermal sensitive materials. However, unlike conventional machining techniques such as turning, milling and grinding in which solid forms of cutting tools are used to machine components to a defined geometry at high accuracy, the performance of AWJ cutting depends strongly on the behaviour of the liquid jet [2–4].

There have been experimental investigations aiming at ''drag reduction'' and improving the ''cohesion'' of a jet by adding cornstarch additives [5–10]. When using this type of liquid in the cutting of various materials with the hardness ranging from ceramic to rubber, it has been reported on a significant increase in the effectiveness of the standard abrasive waterjet by producing narrow kerf widths, reducing abrasive consumption by 50%, and by improving the cutting performance at higher stand-off distances [8]. However, the work included mainly case studies, or the examinations of the pressure profile dropped at different distances from a nozzle [11].

There has not been yet a systematic investigation that accounts quantitatively the relations between the operating parameters and the stability of an additive liquid jet, from which the optimum use of a liquid jet can be achieved. On the other hand, it is noted that the high cost and environmental consciousness due to the large water and chemical consumption are the main factors that have hindered the use of chemical additives widely in high pressure waterjets. These problems become less significant for low-pressure micro-jets that are being developed as an effective technology for precision machining of components used, for example, in micro-electronic devices or biotechnology applications [13,14]. The low volume of liquid consumption and low-pressure apparatus associated with a low-pressure micro-jet enables the operation to be conducted in an enclosed chamber where waste disposal and occupational health and safety (OH&S) issues can be handled with ease.

Furthermore, micromachining requires good jet characteristics such as a high jet stability of the micro-jet for good kerf characteristics on a micro-scale. However, there has been no research on transforming the advance of using cornstarch additive into the micro-jet machining technology.

The phenomenon of liquid jet stability and disintegration to form mist has been studied for several decades. The outcomes have been used in industrial processes, such as the combustion of liquid fuels, gas turbine and food processing where the mist sizes and dispersion patterns are of importance [15,17].In an abrasive dilatant jet (ADJ) with a particular solution containing cornstarch and solid particles, the jet is of non-Newtonian. The variation of viscosity of such slurries significantly affects the stability of an ADJ [17]. An extensive investigation into this issue is of great value for the effective use of this technology. In this paper, an experimental investigation is carried out to provide an understanding of the effect of liquid properties on the stability of an abrasive dilatant jet with cornstarch

additives. A dimensional analysis is then undertaken to develop the mathematical relationship between the jet stability measure and the jetting parameters to provide a practical means for quantitatively predicting the jet stability [18].

2. Experiment

A self-developed ADJ test rig was used for this project, as shown in Fig. 1. The water pressure was controlled by an air-driven Haskel pump with an accumulator to stabilize the pressure. The pressurised water was then injected into a cylinder where it pushed a piston to pass the pressure to the working fluid on the other side of the piston. The water and cornstarch in the cylinder were mixed in cutting head, so that the composition and concentration of the working fluid could be maintained uniformly during the operation. The nozzles were constructed from circular stainless steel tubes, as shown in Fig. 2. The tubes were ground to desired lengths and polished using fine sand paper of 1200 mesh to remove any possible burrs. The nozzle aspect ratio (nozzle length to diameter, l/d) has a significant effect on the initial jet velocity profile. If the ratio is sufficiently large, the boundary layer fills the entire tube, resulting in a fully developed pipe flow.

The experiment was statistically designed considering nozzle diameters (0.84 mm) and water pressures (4MPa). The cornstarch with water composition involved different chemical concentrations (0%, 10%, 22%, by mass), different abrasive particle concentrations (5%, by mass), and particle sizes of 10mm with the mesh number of 1000, respectively. Alumina particles were used. The selection of this chemical was made mainly because its solution within a certain concentration can be disposed easily without a considerable environmental impact. The test conditions are given in Table 1.

Inner contoured regions of the jet, as shown in Figs. 3 and 4 which have higher velocities and are convergent, can result in tapered cuts on the material. The kerf width is dependent on the effective width (or diameter) of the jet, which in turn depends on the jet strength in that zone and the target material.

The primary interests in sheet steel processing are the kerf shape (kerf width and kerf taper) and kerf quality (cut surface roughness) as well as burrs which may be formed at the jet exit. These characteristics will be considered in the present study.

3. Effect of fluid properties

Figs. 5, 6 and 7 shows a typical pattern of the disintegration of a jet at the liquid pressure P = 4MPa and nozzle diameter d = 0.84 mm, when the chemical concentration Cc varied from 0% (pure water), 10% to 22%, respectively. From the analysis of the jets, it has been found.

In Figs. 5, 6 and 7 the effect of traverse speed and different chemical concentrations on width of cut for different material is shown. The cutting speed and chemical concentrations is the most important parameters affecting width of cut. The width of cut diverges as ADJ marches through the specimen at lower traverse speed and converges at higher traverse speed. Thus for lower traverse speed, width of cut is larger at the bottom surface and at higher traverse speed, vice versa [19-21].

The width of cut diverges as ADJ marches through the specimen at lower percentage of cornstarch and converges at higher percentage of cornstarch. Thus for lower percentage of cornstarch, width of cut is larger at the bottom surface and at higher traverse speed, vice versa. These results imply the existence of an optimum traverse speed and percentage of cornstarch to achieve a parallel width. In Fig. 8 the effect of different chemical concentrations on width of cut is shown.

4. Jet kinetic energy

Jet kinetic energy and its variation along and across the jet is an important factor in affecting the jet effective width within which the particles have sufficient energy for material removal. It therefore determines the kerf geometry on the work material. As the kinetic energy of the water within an AWJ is believed to make no contributions to the removal of hard materials like alumina ceramics, only the particle kinetic energy is considered [22,23]. The rate of particle kinetic energy inside an ADJ is given by

$$\frac{dKE}{dt} = \frac{1}{2}(m_a + m_c)v^2 \qquad (1)$$

where m_a is the abrasive mass flow rate, m_c is the cornstarch mass flow rate and v is the particle velocity. In an AWJ, abrasive particles are entrained by the water to increase their velocity. If assuming that the particle has gained the same velocity as its surrounding water at the point of particle impingement on the target material, the particle velocity can be obtained using the following momentum transfer equation [24]:

$$v = \beta_1 \left(\frac{m_w}{m_w + m_a + m_c}\right)v_j \qquad (2)$$

where ψ_1 is the momentum transfer efficiency, v_j is the waterjet velocity, m_w is the water mass flow rate, ma is the abrasive mass flow rate [25,26].

The waterjet velocity from the orifice can be found by the Bernoulli's equation, i.e.

$$v_j = \beta_2 \ \left(\frac{2p}{\rho_w}\right)^{\frac{1}{2}} \tag{3}$$

where ψ_2 is the discharge coefficient, ρ_w is the water density. Substituting Eq. (3) into Eq. (2) gives the particle velocity in relation to water pressure as

$$v = \beta_1 \ \beta_2 \ \left(\frac{m_w}{m_w + m_a + m_c}\right)\left(\frac{2p}{\rho_w}\right)^{\frac{1}{2}} \tag{4}$$

The inclusion of the mass ratio term in Eq. (4) complicates the development of the model. Therefore, to simplify the derivation, the mass ratio term may be approximated to a constant, k_m and Eq. (4) can be re-written as

$$v = \beta_1 \ \beta_2 \ k_m \left(\frac{2p}{\rho_w}\right)^{\frac{1}{2}} \tag{5}$$

$$p = (1 - \varepsilon)p_c \tag{6}$$

where p is the actual water pressure; p_c is pump pressure; ε is water compression coefficient (0.05–0.1) depending on p_c (Olsen, 2005). Substituting Eq. (5) into Eq. (1) yields the equation for the rate of kinetic energy as

$$\frac{dKE}{dt} = \beta_1^2 \beta_2^2 \ k_m^2 \ (m_a + m_c)\left(\frac{p}{\rho_w}\right) \tag{7}$$

The constants in Eq. (7) can be determined by experiments. From this equation, for a given particle mass it is reasonable to represent the effect of particle kinetic energy by water pressure, p, water density, ρ_w, and abrasive mass flow rate, m_a. In addition, kerf geometry is related to the relative position of the jet effective width with respect to the workpiece. Given the characteristics of a jet, this relative position may be considered to relate to the standoff distance, s_d, and the kerf taper compensation angle, α.

5. Jet shear stress model

The aforementioned physical understanding shows that the disintegration of a jet is a result of the internal and external factors and can be analyzed by superimposing the internal disturbances and external disruption. The internal disturbances are associated with the fluid properties and the jet diameter.

The fluid properties comprise dilatant density (ρ_f), surface tension of chemical solution (s), viscosity of chemical solution (m) at the nozzle exit, particle size (d_p) and particle concentration (Cp) for a given particle material [29]. The external disruption is caused by the friction between the jet surface and the atmospheric air which is associated

with the jet velocity or jet pressure (p). For dilatant fluids, a change in jet pressure will result in a change in the liquid properties, i.e. the liquid surface tension and liquid viscosity, which in turn result in a change in the interaction between the internal disturbance and external causes.

Thus, it is possible to develop a model to relate these influencing factors and the jet stability in a general form [31].

$$f(Cp, dp, d, L, p, \rho_f, \sigma, \mu) = 0 \tag{8}$$

where d is the jet diameter at the nozzle exit, L is the jet compact length AB and the other symbols are as defined in Nomenclature.

In forming an ADJ, it is believed that there are energy or momentum losses in the jetting system due to nozzle wall friction, fluid flow disturbances and the compressibility of the dilatant. However, there is a lack of knowledge of the quantitative value of these losses for low-pressure jets at a few mega-pascals. It is believed that these losses for low-pressure dilatant jets can be very small and are ignored in this study. The validity of this approximation will be assessed by examining the predictive capability of the developed model in model verification. Thus, the jet velocity is approximated using the Bernoulli's equation [3], i.e.

$$v = v_j = \beta_2 \ \left(\frac{2p}{\rho_w}\right)^{\frac{1}{2}} \tag{9}$$

where p is the jet pressure and ρ_w are the density of the working fluid which in this case is the dilatant. Following the law of mass conservation, the dilatant density can be determined by

$$\rho_f = \rho_p \frac{v_p}{v} + \rho_c \frac{v_c}{v} + \rho_w \frac{v_w}{v} \tag{10}$$

where ρ_i and ($\frac{v_i}{v}$) is the density and volumetric fraction, respectively; and the subscript (i) for p, c and w denotes the particles, chemical additives and water, respectively. Since the volumes represented by the particles (v_p) and chemical additives (v_c) are very small compared with the overall volume (V), the density of dilatant can be considered uniformly throughout the flow field and is equal to the density of water, i.e.

$$V_c \approx V_w$$

$$\rho = \rho_f = \frac{\rho_c + \rho_w}{2} \tag{11}$$

Thus, Eq. (8) is transformed to:

$$f(Cp, dp, d, L, p, \rho, \sigma, \mu) = 0 \tag{12}$$

For dilatant solutions, the rheological behaviour obeys the power-law model [28-30] which is represented by the following constitutive equation:

$$\tau = k\dot{\gamma}^n \tag{13}$$

For $n < 1$, the fluid exhibits shear-thinning properties,

For $n = 1$, the fluid shows Newtonian behaviour,

For $n > 1$, the fluid shows shear-thickening behavior (dilatant).

where τ is the shear stress, γ is the shear rate, k is the consistency index and n is the flow behaviour index of the dilatant solution. By definition, the shear stress, shear rate and dynamic viscosity have the relation of

$$\mu = \frac{\tau}{\dot{\gamma}} \tag{14}$$

Substituting Eq. (13) into Eq. (14) yields

$$\mu = k\dot{\gamma}^{n-1} \tag{15}$$

Eq. (15) allows the parameters k and n for different chemical concentrations to be determined from the best-fit curves. In the analysis of the flow regimes of dilatants solutions within a solid wall, Valco and Economides [27] stated that beyond a certain distance from the wall where the shear stress is equal to the yield stress of liquid, the stress is not enough to cause a velocity change and the fluid will move as a plug with the uniform velocity. By applying the principle of the force balance between the force driving the flow and the force arising at the outer surface of the liquid body, Valco and Economides[32] then derived the relation between the shear rate ($\dot{Y}$) and the average velocity (V).

According to their analysis, for the flow of power-law fluids characterized by k and n in a circular tube with a diameter d, the relation between the viscosity and the average velocity can be determined by [32,33]

$$\mu(v, k, n) = k\left(\frac{1+3n}{4n}\right)^{n-1}\left(\frac{8v}{d}\right)^{n-1} \tag{16}$$

$$k = \mu\left(\frac{4n}{1+3n}\right)^{n-1}\left(\frac{d}{8\beta_2\,(\frac{2p}{\rho_w})^{\frac{1}{2}}}\right)^{n-1} \tag{17}$$

Substituting Eq. (17) into Eq. (13) yields

$$\tau = \mu\left(\frac{4n}{1+3n}\right)^{n-1}\left(\frac{d}{8\beta_2\,(\frac{2p}{\rho_w})^{\frac{1}{2}}}\right)^{n-1}\dot{\gamma}^n \tag{18}$$

$$\dot{\gamma}_{rz} = \frac{\partial v_r}{\partial z} + \frac{\partial v_z}{\partial r} \tag{19}$$

$$\tau = \tau_{rz} = \mu\left(\frac{4n}{1+3n}\right)^{n-1}\left(\frac{d}{8\beta_2\,(\frac{2p}{\rho_w})^{\frac{1}{2}}}\right)^{n-1}\left(\frac{\partial v_r}{\partial z} + \frac{\partial v_z}{\partial r}\right)^n \tag{20}$$

For this condition (22% cornstarch):

$$\beta_2 = 0.8 \qquad p = 4 Mpa \qquad d = 0.84mm$$
$$\rho_w = 998.2\frac{kg}{m^3} \qquad\qquad n > 1$$
$$\mu = 3.48 \times 10^{-3}\frac{N.S}{m^2} \qquad v = 690\frac{m}{s}$$

$$\emptyset = A \times v = \pi\frac{d^2}{4}v = \pi\frac{(0.84 \times 10^{-3})^2}{4}690 = 379.5 \times 10^{-6}\,m^3s^{-1} \tag{21}$$

$$\tau = \tau_{rz} = 3.48 \times 10^{-3}\left(\frac{4n}{1+3n}\right)^{n-1}\left(\frac{0.84 \times 10^{-3}}{8 \times 0.8(\frac{2 \times 4 \times 10^6}{998.2})^{\frac{1}{2}}}\right)^{n-1}\left(\frac{\partial v_r}{\partial z} + \frac{\partial v_z}{\partial r}\right)^n$$

$$\tau = 3.48 \times 10^{-3}\left(\frac{5.86 \times 10^{-6}n}{1+3n}\right)^{n-1}(\dot{\gamma})^n \tag{22}$$

For (n=2):

$$\tau = \tau_{rz} = 3.48 \times 10^{-3}\left(\frac{5.86 \times 10^{-6} \times 2}{1+3 \times 2}\right)^{2-1}\left(\frac{\partial v_r}{\partial z} + \frac{\partial v_z}{\partial r}\right)^2$$

$$\tau = \tau_{rz} = 5.83 \times 10^{-9}\left(\frac{\partial v_r}{\partial z} + \frac{\partial v_z}{\partial r}\right)^2 = 5.83 \times 10^{-9}\dot{\gamma}^2 \tag{23}$$

For (n=∞):

$$\lim_{n \to \infty} 3.48 \times 10^{-3}\left(\frac{5.86 \times 10^{-6}n}{1+3n}\right)^{n-1}(\dot{\gamma})^n = e^{5344.71}(\dot{\gamma})^n \tag{24}$$

6. Conclusions

An experimental investigation has been carried out to study the non newtonian fluid properties on the jet stability. It has been shown that the liquid viscosity is the major jet internal factor that contributes to the jet cohesion, and the addition of cornstarch additives increased the liquid viscosity and hence the jet stability. By contrast, the jet surface tension that tends to increase the jet cohesion was not increased considerably by the addition of the cornstarch additives. On the other hand, the friction force between the surrounding air and the jet surface promoted break-up of the jet and an increase in the jet pressure decreased the jet stability.

Acknowledgements

References

1. T. Nguyen, D.K. Shanmugam, J. Wang_ School of Mechanical and Manufacturing Engineering, The University of New South Wales, Sydney, NSW 2052, Australia.
2. M. Hashish, A model for abrasive-waterjet (AWJ) machining, Transactions of ASME, 111 (1989) 154–162.

$$A = 0.55 \times 10^{-6}$$

3. J. Wang, Abrasive Waterjet Machining of Engineering Materials, Trans. Tech. Pub., Uetikon-Zuerich, Switzerland, 2003.
4. A. Momber, R. Kovacevic, Principles of Abrasive Waterjet Machining, Springer, 1998.
5. A. White, J. Hemmings, Drag Reduction by Additives-Review and Bibliography, BHRA Fluid Engineering, Cranfield, Bedfordshire, UK, 1976.
6. G.W. Howells, Polymer blasting with super-water from 1974 to 1989: a review, International Journal of Waterjet Technology, 1 (1990), 1–16.
7. R. Hollinger, W. Perry, R. Swanson, Precision cutting with a low pressure, coherent abrasive suspension jet, in: The 5th American Waterjet Conference, Toronto, Canada, 1989, pp. 245–252.
8. J. Zakin, D. Summers, The effect of visco-elastic additives on jet structure, in: The 3rd International Symposium on Jet Cutting Technology, Chicago, 1976, pp. A4-47–A4-66.
9. S. Chacko, A. Gupta, D. Summers, Comparative performance study of polycrylamide and xanthum polymer in abrasive slurry jet, in: American Waterjet Conference, Houston, TX, 2003, p. 5-C.
10. H. Louis, F. Pude, C. von Rad, Potential of polymeric additives for the cutting efficiency of abrasive waterjets, in: WJTA American Waterjet Conference, Houston, TX, 2003, p. 3-D.
11. H. Liu, J. Wang, N. Kelson, R.J. Brown, A study of abrasive waterjet characteristics by CFD simulation, Journal of Materials Processing Technology 153/154 (2004), 488–493.
12. D. Summers, Waterjetting Technology, Chapman & Hall, 1984.
13. D.S. Miller, Micromachining with abrasive waterjets, Journal of Materials Processing Technology 149 (1–3) (2004), 37–42.
14. Y. W. Lee, T. L. Chang, F. H. Ko, S. H. Chang, C. C. Chen, Experimental and theoretical analysis of microjet droplet behavior, Microelectronic Engineering 84 (5–8) (2007), 1770–1774.
15. L. Bayvel, Z. Orzechowski, Liquid Atomization, Combustion-An International Series, Taylor & Francis, 1993.
16. [16] Y. I. Khavkin, Theory and Practice of Swirl Atomizers, Taylor & Francis, 2004.
17. A. H. Lefebvre, Atomization and Spray, Combustion-An International Series, Hemisphere Pub. Corp., 1989.
18. M.J. McCarthy, N.A. Molloy, Review of stability of liquid jets and the influence of nozzle design, The Chemical Engineering Journal 7 (1) (1974), 1–20.
19. T. Nguyen, L.C. Zhang, Modelling of the mist formation in a segmented grinding wheel system, International Journal of Machine Tools and Manufacture 45 (1) (2005), 21–28.
20. T. Nguyen, L.C. Zhang, The coolant penetration in grinding with segmented wheels-Part 1: Mechanism and comparison with conventional wheels, International Journal of Machine Tools and Manufacture 45 (12/13) (2005), 1412–1420.
21. S. Matsumoto, Y. Takashima, Atomization characteristics of power law fluids by rotating disks, in: The 1st International Conference on Liquid Atomization and Spray Systems (ICLAS'78), Tokyo, Japan, 1978, pp. 145–150.
22. R.P. Grant, S. Middleman, Newtonian jet stability, Journal for the American Institute of Chemical Engineers 12 (4) (1966), 669–678.
23. Y. Kitamura, T. Takahashi, Stability of a liquid jet in air flow normal to the jet axis, Journal of Chemical Engineering, Japan 9 (4) (1976), 282–286.
24. D.K. Shanmugam, J. Wang _, H. Liu School of Mechanical and Manufacturing Engineering, The University of New South Wales, Sydney, NSW 2052, Australia.
25. N. Dombrowski, W.R. Johns, The aerodynamic instability and disintegration of viscous sheets, Chemical Engineering Science 18 (1963), 203–214.
26. J. Zhang, R. Pelton, The surface tension of aqueous poly (Nisopropylacrylamide- co-acrylamide), Journal of Polymer Science: Part A: Polymer Chemistry 37 (1999), 2137–2143.
27. P. Valko, M. Economides, Hydraulic Fracture Mechanics, Wiley, 1995.
28. [28] R. Tanner, Engineering Rheology, second ed., Oxford University Press, New York, 2000.
29. E. A. Samia, Synthesis of copolymeric hydrogels using gamma radiation and their utilization in the removal of some dyes in wastewater, Journal of Applied Polymer Science, 102 (4) (2006), 3720–3731.
30. M. B. Karamis, Tribology at high-velocity impact, Tribology International, 40 (1) (2007), 98–104.
31. L. Bayvel, Z. Orzechowski, Liquid Atomization, Combustion—An International Series, Taylor & Francis, 1993.
32. P. Valko, M. Economides, Hydraulic Fracture Mechanics, Wiley,1995.
33. R. Tanner, Engineering Rheology, second ed., Oxford UniversityPress, New York, 2000.
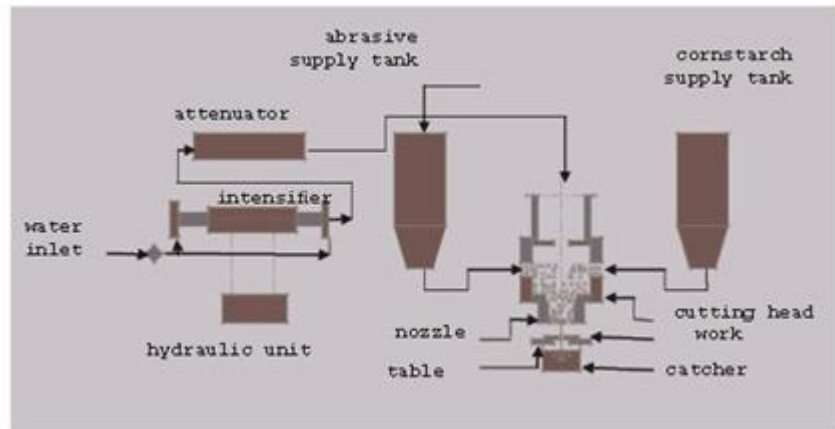
1/29/2013

Appendix

Figure 1. General layout of an abrasive type dilatantjet cutting system with cornstarch supply tank
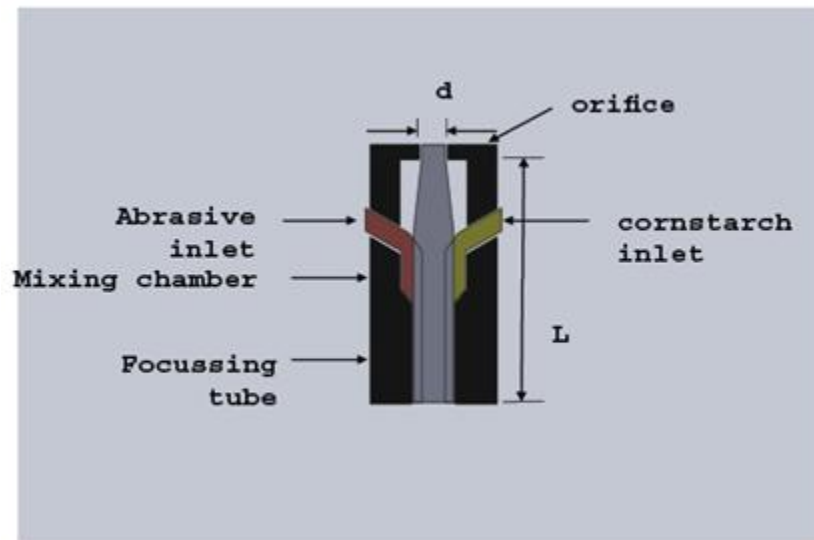

Figure 2. Construction of an abrasive & cornstarch injection nozzle
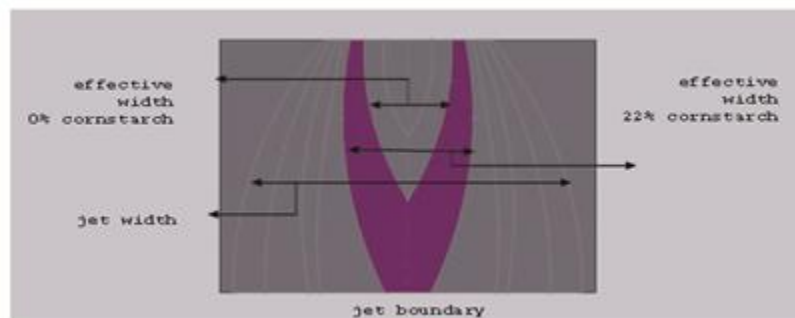

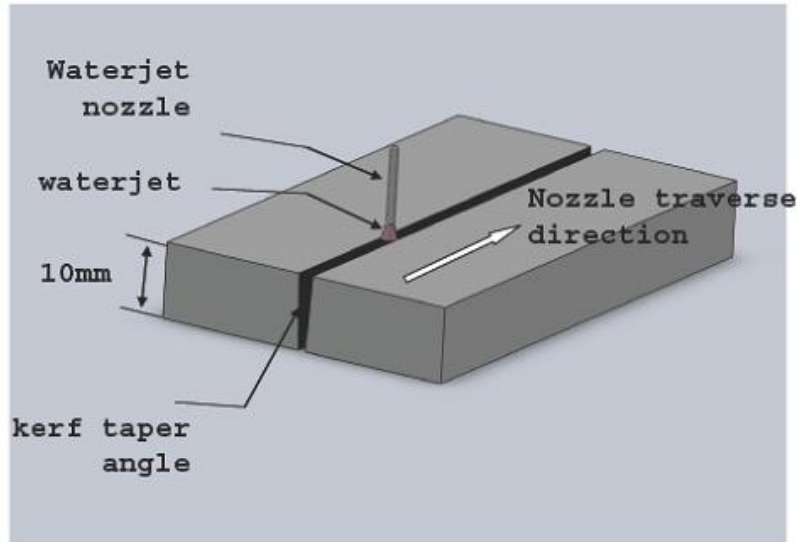
Figure 3. Relative strength zones in a dilatantjet

Figure 4. Abrasive dilatantjet cutting of composites showing the kerf taper formation
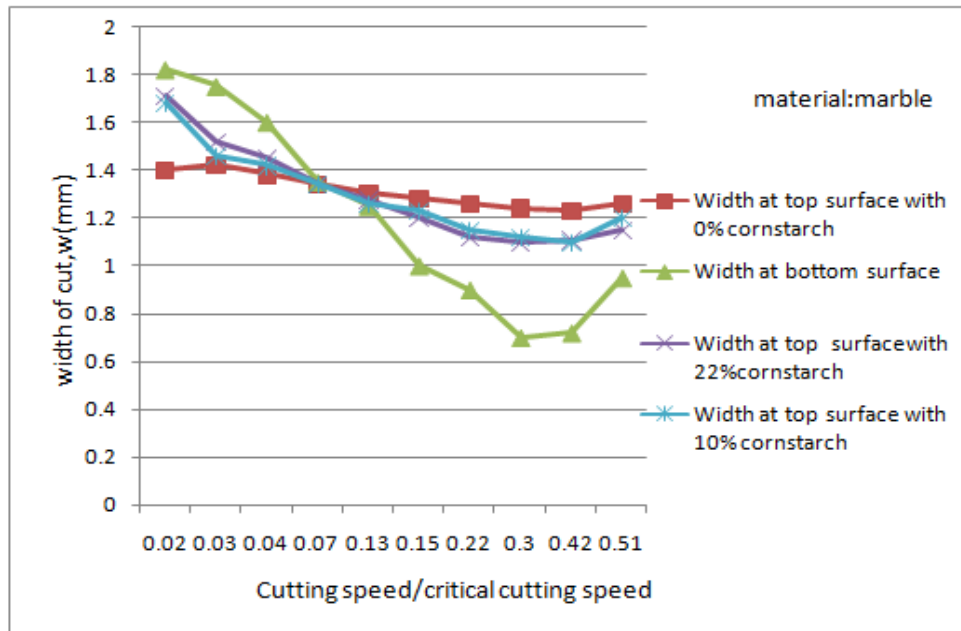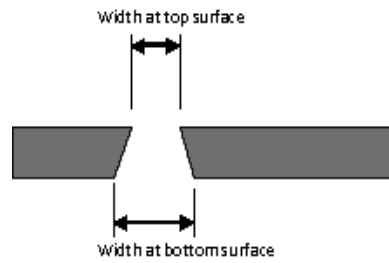

Figure 5. Effect of traverse speed and different chemical concentrations on width of cut
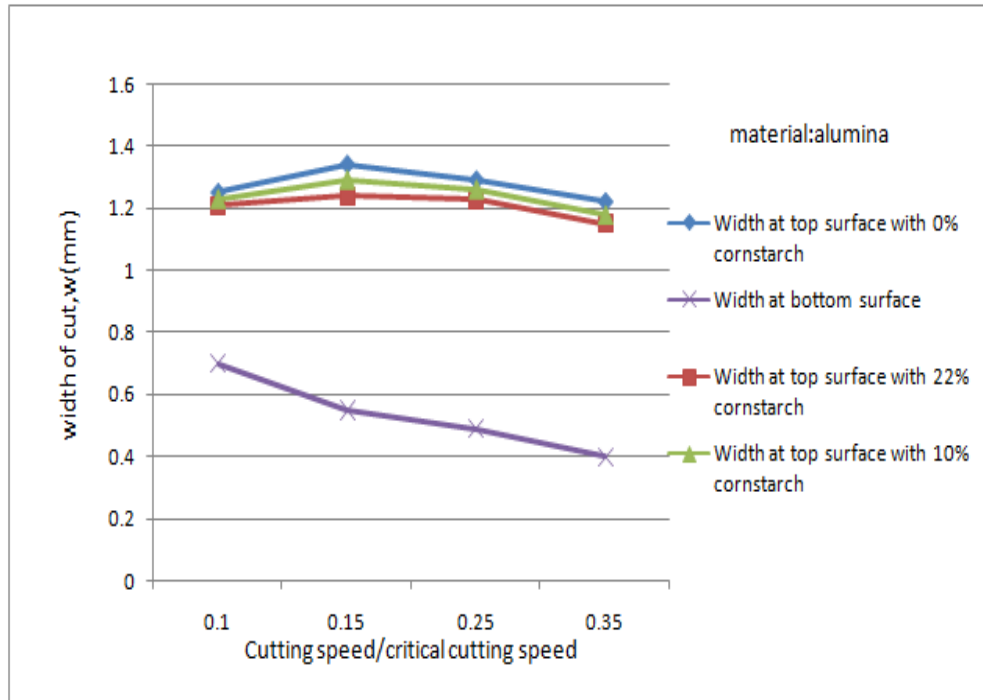
Figure 6. Effect of traverse speed and different chemical concentrations on width of cut
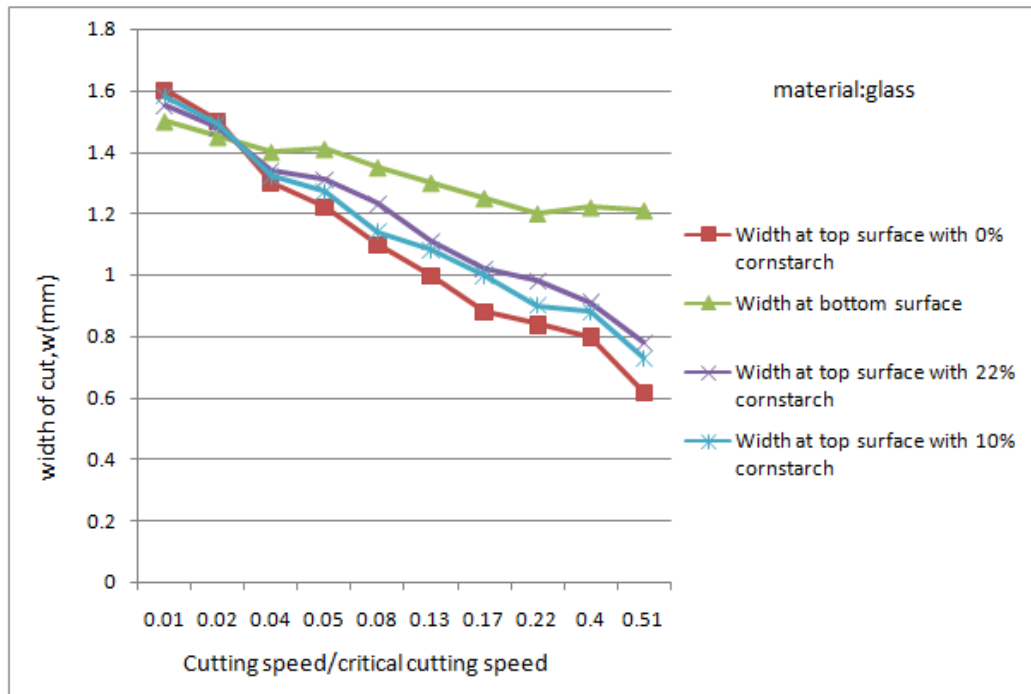

Figure 7. Effect of traverse speed and different chemical concentrations on width of cut
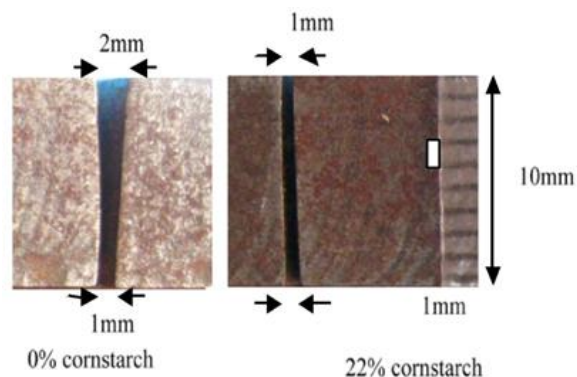
Figure 8. Material cut at two different chemical concentrations

Table 1. Experimental parameter

Nozzel diameter(mm)	0.84
Pressure(Mpa)	400 Mpa
Dilatant composition	
Cornstarch additive(%,mass)	0 (water only),10,22
Alumina particle(%,mass)	5
Particle mesh number(and size in brackets	#1000 (dp=10μm)

Table 2. Experimental parameters (material: marble)

Cutting speed/critical cutting speed	Width at top surface with 0% cornstarch	Width at bottom surface	Width at top Surface with 22%cornstarch	Width at top surface with 10% cornstarch
0.02	1.40	1.82	1.71	1.68
0.03	1.42	1.75	1.52	1.46
0.04	1.38	1.60	1.45	1.42
0.07	1.34	1.35	1.34	1.34
0.13	1.30	1.25	1.28	1.26
0.15	1.28	1.00	1.20	1.23
0.22	1.26	0.90	1.12	1.15
0.30	1.24	0.70	1.1	1.12
0.42	1.23	0.72	1.11	1.10
0.51	1.26	0.95	1.15	1.20

Table 3. Experimental parameters (material: alumina)

Cutting speed/critical cutting speed	Width at top surface with 0% cornstarch	Width at bottom surface	Width at top surface with 22% cornstarch	Width at top surface with 10% cornstarch
0.10	1.25	0.70	1.21	1.23
0.15	1.34	0.55	1.24	1.29
0.25	1.29	0.49	1.23	1.26
0.35	1.22	0.40	1.15	1.18

Table 4. Experimental parameters (material: glass)

Cutting speed/critical cutting speed	Width at top surface with 0% cornstarch	Width at bottom surface	Width at top surface with 22% cornstarch	Width at top surface with 10% cornstarch
0.01	1.60	1.50	1.55	1.58
0.02	1.50	1.45	1.48	1.49
0.04	1.30	1.40	1.34	1.32
0.05	1.22	1.41	1.31	1.27
0.08	1.10	1.35	1.23	1.14
0.13	1.00	1.30	1.11	1.08
0.17	0.88	1.25	1.02	1.0
0.22	0.84	1.20	0.98	0.9
0.40	0.80	1.22	0.91	0.88
0.51	0.62	1.21	0.78	0.73